

# Accepted Manuscript

Part-Load characteristics of a new ammonia/lithium nitrate absorption chiller

Miguel Zamora , Mahmoud Bourouis , Alberto Coronas , Manel Vallès

PII: S0140-7007(14)00303-X

DOI: [10.1016/j.ijrefrig.2014.11.005](https://doi.org/10.1016/j.ijrefrig.2014.11.005)

Reference: JIJR 2919

To appear in: *International Journal of Refrigeration*

Received Date: 1 July 2014

Revised Date: 3 November 2014

Accepted Date: 5 November 2014

Please cite this article as: Zamora, M., Bourouis, M., Coronas, A., Vallès, M., Part-Load characteristics of a new ammonia/lithium nitrate absorption chiller, *International Journal of Refrigeration* (2014), doi: 10.1016/j.ijrefrig.2014.11.005.

This is a PDF file of an unedited manuscript that has been accepted for publication. As a service to our customers we are providing this early version of the manuscript. The manuscript will undergo copyediting, typesetting, and review of the resulting proof before it is published in its final form. Please note that during the production process errors may be discovered which could affect the content, and all legal disclaimers that apply to the journal pertain.



**Part-Load characteristics of a new ammonia/lithium nitrate absorption chiller****Miguel Zamora<sup>a</sup>, Mahmoud Bourouis<sup>b\*</sup>, Alberto Coronas<sup>b</sup>, Manel Vallès<sup>b</sup>**

<sup>a</sup> *CIAT Air Thermodynamics R&D Department. Pol. Llanos de Jarata s/n 14550 Montilla, Córdoba, Spain*

<sup>b</sup> *Department of Mechanical Engineering, Universitat Rovira i Virgili, Av. Països Catalans No. 26, 43007 Tarragona, Spain*

\* *Corresponding Author (Email: [mahmoud.bourouis@urv.cat](mailto:mahmoud.bourouis@urv.cat); Phone: +34 977 55 86 13; Fax: +34 977 55 96 91)*

**Abstract**

A pre-industrial prototype of a new water-cooled ammonia/lithium nitrate absorption chiller was characterised at part-load operation mode. The chiller was built using brazed plate heat exchangers in all its components, including the absorber and the generator.

A test campaign was carried out varying the thermal load in the chilled water circuit and keeping the hot and cooling water temperatures constant.

Part-load curves of the thermal and electrical coefficients of performance were obtained, plotted and compared with data from the literature on small capacity absorption chillers with conventional working pairs, namely ammonia/water and water/lithium bromide. The experimental results showed that to achieve a higher electrical coefficient of performance at part-load operation, it was much more convenient to use an ON-OFF control than to modify the hot water temperature. Furthermore, using a simple ON-OFF control strategy, the behaviour of the new absorption chiller was more agile and responded more quickly.

The part-load curve of the electrical coefficient of performance was obtained by adjusting the experimental data to the shape of the curve proposed in the standard prEN-14511:2011 for air-to-water chillers. The  $C_c$  coefficient was 0.7985 matching the value obtained dividing the remaining electrical consumption measured during the OFF half cycles by the total energy consumption generated.

**Keywords:** Absorption chiller, ammonia, lithium nitrate, part-load operation, control

### Nomenclature

BPHE: brazed plate heat exchanger

$COP_{ther}$ : thermal coefficient of performance

$COP_{elec}$ : electrical coefficient of performance

P: pressure (bar)

$\dot{Q}$ : thermal power (kW)

T: temperature (°C)

PLR: part-load ratio =  $\frac{\dot{Q}_C}{\dot{Q}_{EN}}$

$P_w$ : electrical power input (kW)

### Subscripts

1: inlet to the chiller (\*)

2: outlet to the chiller (\*\*)

AC: absorber/condenser

E: evaporator/evaporation

G: generator/generation

C: cooling load

hyd: hydraulic power

N: full capacity

w: water side

(\*) When not indicated,  $T_E$  denotes chilled water outlet temperature

(\*\*) When not indicated,  $T_G$ ,  $T_{AC}$ , denote temperatures at the chiller inlet

#### *Greek letters*

$\dot{v}$ : volumetric flow rate ( $\text{m}^3 \cdot \text{h}^{-1}$ )

$\Delta P$ : pressure drop (bar)

$\Delta T$ : temperature difference ( $^{\circ}\text{C}$ )

$\eta$ : pump efficiency

$\Pi$ : period. Interval of time for a steady state cycle

n: number of selected periods considered for energy integration

#### **Introduction**

In the last 50 years there have been several studies that have analysed the control of large-scale absorption chillers (Mann and Stewart 1963, Anderson 1966, Ogawa et al. 1992, Yeung et al. 1992, Koepfel et al. 1995, Chow et al. 2002, Jenkins 2003, Pérez de Viñaspre et al. 2004 and Park et al. 2004). The control of these large-scale absorption chillers is usually obtained by the use of a capacity valve in the hot medium circuit.

Two variants of this control are currently the most common. The first variant consists of modulating the heat medium (usually steam or hot water) flow from 10 to 100%. The second variant is achieved by adjusting the heat medium temperature at the inlet. Either of these modulating techniques used in conjunction with internal control of solution flow rate itself achieved by variable frequency drives, enables faster chiller response time to the changing thermal load and the cooling medium conditions (Labus et al. 2012). However, recently published works (Yeung et al. 1992, Koeppel et al. 1995, Chow et al. 2002, Park et al. 2004) have also included the control of the cooling tower as a way of reducing power consumption.

In contrast to large-scale absorption chillers, which have been available on the market for a long time, the interest for small-scale absorption chillers has only recently arisen. This is due to the increasing interest in the introduction of solar cooling systems and the reduction of electricity consumption. With only a few commercial units and with scarce research done yet in this field, the control issues are still in the development phase. Most papers published are based on the results of theoretical simulations which used the characteristic equation model to estimate the performance of the absorption chiller at the different thermal conditions of the external circuits (Storckenmaier et al. 2003, Clauß et al. 2007, Albers et al. 2008, Kühn et al. 2008).

The catalogues of the commercial units (Rotartica, 2007; Chilli, 2008; Yazaki, 2009) show that most small capacity absorption chillers are controlled by a simple ON-OFF control switch. When the absorption chiller is started up, it remains in operation as long as there is a demand for cooling. The hot water circuit pump or bypass valve is cycled ON and OFF to control the flow of the hot water supply to the generator in response to the chilled water temperature.

Lazzarin (1980, 2007a, 2007b) studied the performance at a steady state and transient state of two water/lithium bromide units of 4.5 kW and 25 kW. The chillers were equipped with a vapour-lift pump. The analysed units had an ON-OFF control that was described by the author as unsatisfactory. The system start-up time took 30 minutes because, until the heat energy supplied to the generator ensured the first boiling of the refrigerant and the absorption began, there was no frigorific effect, so a prolonged stop just after a start-up can waste all the heat energy supplied to the chiller. Lazzarin analysed the results at part-loads of 25%, 50% and 75% and concluded that the thermal coefficient of operation ( $COP_{ther}$ ) was heavily penalized. For instance, for a test with 50% load and one cycle per hour (30 minutes ON and 30' OFF), the cooling capacity was reduced by 60% and the accumulated  $COP_{ther}$  dropped by 36%, which is considered an unacceptable penalty for part-load operation. Finally as a more suitable control method, the author suggested varying the hot water flow in the generator to regulate the cooling capacity.

Didion and Radermacher (1984) performed an experimental study on the part-load operation of a 10 kW gas-fired absorption chiller using ammonia/water as a working pair and a dry coil for dissipating the heat released in the absorber and condenser. The unit had an ON-OFF control so that during the part load tests the machine operated according to starting and stopping cycles. The data analysis technique was based on the representation of the thermal coefficient of performance ( $COP_{ther}$ ) versus the part load ratio (PLR). For a PLR of 20%, the  $COP_{ther}$  was equal to 74% of the full capacity value (coefficient of degradation  $C_d = 0.74$ ). The explanation for this loss in the performance was directly related to the design of the absorption machine. In the case of the machine analysed by Didion and Radermacher (1984) the absorber was of the falling film type and it was the limiting component during the start-up phase in each ON half cycle. The

explanation given by the authors was that the generator accumulated the weak solution and during the OFF half cycle this migrated back to the absorber which was flooded thus delaying the heat and mass transfer processes when a new ON half cycle was started. Furthermore, there was a heat pipe effect between the high temperature and low temperature zones which altered the movement of the fluids during the OFF half cycles. They proposed the incorporation of shut-off valves to isolate the migration of refrigerant and solution from the condenser to the evaporator and from the generator to the absorber respectively. With this measure and at a PLR of 20%, the  $COP_{ther}$  reached 89% of the full capacity value.

One of the conclusions which can be drawn from the existing literature is that, although ON-OFF operation of the external circuits is simple to install and to operate, this control strategy should be avoided in commercial machines. In fact, this control strategy causes the system performance to decrease due to the frequency of the ON-OFF cycles of the chiller and therefore cannot be justified only by its simplicity. In other words, a mass flow and/or temperature control should be installed in the external circuits. Moreover, to achieve maximum efficiency, small absorption machines should operate continuously at full load.

A new absorption chiller of 10 kW of cooling capacity using the ammonia/lithium nitrate fluid mixture was developed by CIAT in collaboration with the CREVER research group of the Rovira i Virgili University. A comparison of the advantages and disadvantages of ammonia/lithium nitrate with the conventional working pairs used in absorption chillers was reported by the authors in Zamora et al. (2014).

During 2010 and 2011 two pre-industrial prototypes, an air-cooled one and a water-cooled one, were manufactured and tested (Zamora et al. 2014). In a first test campaign, the cooling capacity and the thermal and electrical coefficients of performance ( $COP_{ther}$

and  $COP_{elec}$ ) were determined from experimental measurements. Cooling capacity and generation power were also correlated by multivariate linear regression as a function of the external source temperatures (Zamora 2012).

The new absorption chiller is a single-effect unit, built using brazed plate heat exchangers (BPHEs) in all its thermal components including the generator and the absorber (Bourouis et al. 2009). This design offers dynamic behaviour different to other absorption chillers, especially those that use water/lithium bromide as a working pair and which require larger heat exchangers with greater thermal inertia.

The objective of this paper is to determine the performance characteristics of the water-cooled prototype at part-load operation. Special attention will be paid to the degradation of the electrical coefficient of performance ( $COP_{elec}/COP_{elecN}$ ) at part-load since the literature review showed that the previous works were mainly focused on the thermal coefficient of performance. The study will examine whether the construction based on plate heat exchangers reduces thermal inertia in the chiller and if this has any effect on the strategies employed to control the machine.

### **Part load test standards**

There is no specific standard for testing the new ammonia/lithium nitrate absorption chiller so different existing norms were considered.

The standard ANSI/ARI 560-2000 entitled “*Absorption Water Chilling and Water Heating Packages*” establishes a procedure for testing water-cooled single-effect water/lithium bromide absorption chillers driven by hot water. Another possibility would be to follow, where applicable, the standard prEN 14825:2011 entitled “*Air conditioners, liquid chilling packages and heat pumps, with electrically driven*

*compressors, for space heating and cooling – Testing and rating at part load conditions and calculation of seasonal performance”.*

The approach proposed in these standards is based on the calculation of the *Integrated Part-Load Value (IPLV)* in the case of ANSI/ARI 560-2000 or the *Seasonal Energy Efficiency Ratio (SEER)* in the case of prEN 14825:2011. These seasonal energy efficiency ratios are calculated as a weighted average of four values of the coefficient of performance (COP) and are measured at four operating conditions (PLR= 100%;  $T_{AC1}= 35\text{ }^{\circ}\text{C}$ ), (PLR= 75%;  $T_{AC1}= 30\text{ }^{\circ}\text{C}$ ), (PLR=50%;  $T_{AC1}= 22\text{ }^{\circ}\text{C}$ ) and (PLR= 25%;  $T_{AC1}= 18\text{ }^{\circ}\text{C}$ ). It must be noted that the measured COP values can not be used to plot the part-load degradation curve of the coefficient of operation directly because they depend on both PLR and  $T_{AC1}$  at the same time.

The second remarkable aspect is that the chiller capacity control was set manually for every test condition. For instance, in the case of absorption chillers, if the variable capacity of the machine was controlled by means of variable generation temperature, the test was conducted supplying the exact generation temperature necessary to obtain the required part-load and fixing the chilled water supply and the chilled water temperature difference ( $\Delta T$ ). In the case of vapour compression chillers, if the tested machine had more than one compressor, the test was conducted by running just the required number of them. By doing this, each part-load test was conducted as a full capacity test, keeping the unit running at steady state conditions. The different operation variables were measured and registered and at given intervals of time and time-average values were then calculated. In other words, the chiller was not left freely to auto-control.

In the cases where the chiller control is of the ON-OFF type or where the part-load level is lower than the minimum capacity level and the chiller has to cycle, the standards

propose the use of a part-load cycling degradation curve of the thermal coefficient of operation ( $COP_{ther}$ ). The expression of this curve, which is implicitly formulated in the ANSI/ARI 560-2000 standard, is (Eq. (1)):

$$\frac{COP_{ther}(T_{AC}, T_E, T_G, PLR)}{COP_{ther}(T_{AC}, T_E, T_G)|_{PLR=100\%}} = \frac{1}{1.13 - 0.13 \cdot PLR} \quad (1)$$

In the case of the standard prEN 14825:2011 for vapour compression machines, the part-load curves are formulated in Eq. (2) and Eq. (3):

$$\frac{COP_{elec}(T_{AC}, T_E, T_G, PLR)}{COP_{elec}(T_{AC}, T_E, T_G)|_{PLR=100\%}} = \frac{PLR}{(1 - Cc) + Cc \cdot PLR} \quad (2)$$

$$\frac{COP_{elec}(T_{AC}, T_E, T_G, PLR)}{COP_{elec}(T_{AC}, T_E, T_G)|_{PLR=100\%}} = 1 - Cd \cdot (1 - PLR) \quad (3)$$

The expression in Eq. (2) was proposed for water-to-water and air-to-water chillers, while the expression in Eq. (3) was proposed for air-to-air and water-to-air air-conditioners. These two expressions were reported in classical DOE publications like Henderson et al., 1999. The standard prEN 14825:2011 establishes that, if no test is performed, the coefficients Cc and Cd can be taken as 0.9 and 0.75 by default, respectively.

Figure 1 shows the graphical representation of equations (1), (2), and (3).

### Test bench description

In order to test the new ammonia/lithium nitrate absorption chiller with an ON-OFF control at part-load capacity, the test bench of the CREVER Laboratory at University Rovira i Virgili was modified by adding an inertia water tank of 150 l (Fig. 2). This meant that the chilled water circuit was a closed circuit and could simulate the inertia in

the actual building distribution network. The variable cooling load was provided thanks to a plate heat exchanger. A by-pass valve, commanded by a PID control, set the cooling load by maintaining a certain  $\Delta T_C$  ( $T_{C1}-T_{C2}$ ) in the plate heat exchanger.

Temperatures were measured with Pt-100 of  $\pm 0.1$  K precision at every inlet and outlet chiller pipe. Three flow meters of  $\pm 0.5\%$  precision were installed in every water circuit. The uncertainty of measurement of the cooling capacity and the generation power was 0.5 kW.

### **Test procedure**

The water-cooled pre-industrial prototype (PRE\_IND\_W\_W) was installed on the test bench (Fig. 2). A fixed hot water inlet temperature ( $T_{Gi}$ ) and a fixed cooling water inlet temperature ( $T_{AC1}$ ) were set by means of the controls on the test bench.

Every time the solution pump was on, the refrigerant electronic expansion valve and a solenoid valve located in the poor solution line were also on. There was also a check valve at the solution pump discharge to prevent backflow. With these three components, refrigerant and solution migration from the high pressure side to the low pressure side was avoided.

The chilled water pump was always running. However, the generation water pump, and the cooling water pump only ran at the same time as the solution pump did. The operation of these two pumps was controlled by the chiller regulation.

The chilled water outlet temperature ( $T_{E2}$ ) was controlled by the chiller regulation. In a first experimental campaign, the start of the absorption process was established at  $T_{E2}$  equal to  $18^\circ\text{C}$  and the stop of the absorption was set at  $T_{E2}$  equal to  $13^\circ\text{C}$ , thus the average chilled water outlet temperature was  $15.5^\circ\text{C}$ .

The test procedure was as follows:

1. Water flow rates were set according to Table 1. A discussion about the influence of the water flow rates on the operation of the ammonia/lithium nitrate prototype had been reported by the authors in Zamora et al. (2014)
2. Prototype did not include circulation pumps, so pressure drop ( $\Delta P$ ) was measured in each water circuit in order to carry out the corrections in the electric power absorbed and in the cooling capacity according to the standard prEN 14511-3:2011 (Table 2).
3. Average chilled water outlet temperature set point was established in the absorption chiller control according to Table 1.
4. Scanning rate was set to 5 seconds in the data acquisition system.
5.  $T_{GI}$  and  $T_{AC1}$  values were set in the test bench control system according to Table 1.
6. The absorption chiller was set ON (from the stand-by mode).
7. A full capacity test was carried out to determine the full load temperature difference  $\Delta T_{CN}$ . Full cooling capacity was also obtained ( $\dot{Q}_{EN}$ ).
8. For every part-load test, the load compensation PID control needed to be adjusted in order to maintain the follow temperature differences:

$$75\%: \Delta T_C = T_{C1} - T_{C2} = 0.75 \cdot \Delta T_{CN}$$

$$50\%: \Delta T_C = T_{C1} - T_{C2} = 0.50 \cdot \Delta T_{CN}$$

$$25\%: \Delta T_C = T_{C1} - T_{C2} = 0.25 \cdot \Delta T_{CN}$$

9. Temperatures and water flows were recorded and the operation ON-OFF cycles are monitored.

10. Power consumption of the chiller was recorded.
11. The cooling effect delivered by the chiller was obtained integrating the cooling capacity throughout a selected number of steady state periods ( $n \cdot \Pi$ ). This value was reduced by subtracting the chilled water pump energy consumption value calculated in step 15.
12. The actual PLR was obtained dividing the actual cooling energy by the maximum energy that the unit could have given, which was  $\dot{Q}_{EN} \cdot n \cdot \Pi$ .
13. The generation energy was obtained integrating the generation power throughout the selected number of steady state periods ( $n \cdot \Pi$ ).
14. The chiller electrical energy consumption was obtained integrating the chiller power consumption throughout the selected number of steady state periods ( $n \cdot \Pi$ ). This value was increased by adding the pump's electrical energy consumption calculated as indicated in steps 15 and 16.
15. The chilled water pump electrical energy consumption to be subtracted from the cooling energy and added to the chiller electrical energy consumption was the integral of power given in Table 2 throughout the selected number of steady state periods ( $n \cdot \Pi$ ).
16. Electrical energy consumptions of the generation and cooling water pumps, to be added to the chiller electrical energy consumption was the integral of the power values given in Table 2 throughout the ON half time of the selected number of steady state periods.
17. The values of the thermal ( $COP_{ther}$ ) and electrical ( $COP_{elec}$ ) coefficients of performance at each part-load were calculated as the ratio of the cooling energy

relative to the generation energy and the chiller total electrical energy consumption respectively.

A further test was carried out at a lower chilled water outlet temperature ( $T_{E2} = 8.5 \text{ }^\circ\text{C}$ ) in order to assess the COP degradation values at different operating conditions.

### Test results and discussion

Table 3 shows the results at full load. The electric consumptions of the hot and cooling water circulation pumps are very relevant as evidenced by the reduction of the  $\text{COP}_{\text{elec}}$  (prEN 14511-3:2011), calculated in accordance with the standard prEN 14511-3:2011. It must be remarked that the control system and chilled water pump were permanently consuming energy, even during the OFF half cycles.

Figure 3 shows the temperature profiles recorded during 3 stable cycles for the 50% load test at  $15.5 \text{ }^\circ\text{C}$  chilled water outlet temperature. While  $\Delta T_C$  is kept constant by the PID control emulating the cooling load,  $\Delta T_E$  varies as it would do in an actual installation due to the decoupling effect created by the inertia tank.

In Figure 4 the cooling load ( $\dot{Q}_C$ ), the cooling capacity ( $\dot{Q}_E$ ) and the generation power ( $\dot{Q}_G$ ) are plotted. The ON-OFF cycles of  $\dot{Q}_E$  and  $\dot{Q}_G$  can be observed, while the cooling load  $\dot{Q}_C$  is kept constant. The quick response of the unit is worthy of note and very similar to that of the vapour compression chillers. This is one of the major advantages of the new development that uses Braze Plate Heat Exchangers (BPHEs) in all the thermal components.

Figures 5 and 6 show the temperature profiles and thermal loads achieved at 50% PLR for the test at  $8.5 \text{ }^\circ\text{C}$  chilled water outlet temperature. The first fifteen minutes show the

data recorded with the machine operating at full load. Again, it can be seen how, after each new start the machine reached full capacity within a few minutes.

Tables 4 and 5 present the cooling energy values produced by the chiller, the thermal energy input to the generator, the electrical energy consumed by the chiller and external pumps and also, the resulting thermal and electrical COPs obtained for the tests at 15.5 °C and 8.5 °C chilled water outlet temperature, respectively.

Table 6 summarises all the tests conducted and presents the degradation values defined as the actual COP values divided by full capacity COP value.

As seen in Figure 7, taking into account the uncertainty in measurement, the degradation values of the thermal coefficient of performance ( $COP_{ther}$ ) obtained in the present work are of the same order of magnitude as the data reported by Didion and Radermacher (1984). The new ammonia/lithium nitrate absorption chiller presents slightly worse behaviour than the ammonia/water chiller. This can be explained by the higher viscosity of the solution which causes higher losses due to the inertia at every new start up and also because the unit tested by those authors was an air-cooled unit which at each OFF half cycle still continued dissipating the condensation and absorption heat in the coil.

Regarding the electrical coefficient of performance ( $COP_{elec}$ ), the coefficient  $C_c$  of Eq. (2) was adjusted using the method of least squares and taking the values from Table 6. The mathematical expression of the corresponding part-load curve is given in Eq. (4). The degradation curve with the obtained coefficient  $C_c$  plotted against experimental values is shown in Figure 8.

$$\frac{COP_{elec}(T_{AC}, T_E, T_G, PLR)}{COP_{elec}(T_{AC}, T_E, T_G)|_{PLR=100\%}} = \frac{PLR}{(1 - 0.7985) + 0.7985 \cdot PLR} \quad (4)$$

It is worth mentioning that the value of  $C_c$  obtained by this method matches the value of  $C_c$  obtained by simply dividing the remaining amount of electricity consumed during the OFF half cycles by the total consumption as suggested in the prEN 14825:2011 for water-to-water vapour compression chillers. During the OFF half cycle the only consuming elements were the control system (80 W) and the chilled water pump (79 W) which represented a 159 W consumption in total. During the ON half cycle the total consumption was 784 W (Table 3). So  $C_c = 1 - (159 / 784) = 0.7972$ . This indicates the similarity between the behaviour at part-load of the new ammonia/lithium nitrate absorption chiller and the usual response of a conventional mechanical compression chiller.

### Capacity control

It is also worthwhile making a comparison between the use of the ON-OFF control or the standard control which varies the hot water temperature ( $T_G$ ) in the absorption machine being tested.

When the cooling capacity is controlled to adapt it to the thermal load, Eq. (5) shows that the actual electrical coefficient of performance ( $COP_{elec}$ ) divided by the full capacity electrical coefficient of performance ( $COP_{elecN}$ ) is always equal, by definition, to the part-load ratio (PLR) whatever the temperatures  $T_G$  chosen, since the electrical power  $P_w$  is constant.

$$\frac{COP_{elec}(T_{AC}, T_E, T_G, PLR)}{COP_{elec}(T_{ACN}, T_{EN}, T_{GN})|_{100\%}} = \frac{\frac{\dot{Q}_E(T_{AC}, T_E, T_G, PLR)}{P_w}}{\frac{\dot{Q}_E(T_{ACN}, T_{EN}, T_{GN})|_{100\%}}{P_w}} = \frac{\dot{Q}_E(T_{AC}, T_E, T_G, PLR)}{\dot{Q}_E(T_{ACN}, T_{EN}, T_{GN})|_{100\%}} = PLR \quad (5)$$

Figure 9 shows a plot of the degradation curve adjusted from the part-load tests when the cooling capacity was controlled using the ON-OFF approach (Eq. (4)), and the degradation curve (diagonal  $y = \text{PLR}$ ) was obtained when controlling the cooling capacity by modifying the hot water temperature according to Eq. (5).

As seen in Figure 9, when operating at part-load ( $\text{PLR} < 100\%$ ), an ON-OFF control is much more appropriate than to modify the  $T_G$ . For cases of high cooling demand with a PLR above 100%, Figure 9 also shows that the higher the hot water temperature, the higher the electrical coefficient of performance ( $\text{COP}_{\text{elec}}$ ). It will thus always be more suitable to operate at the maximum hot water temperature available, limited by a safety value.

The capacity control based on modifying the hot water flow rate must be discarded because it presents a small margin of modulation. According to previous measurements (Zamora et al. 2014), reducing the hot water flow a 50%, from  $3 \text{ m}^3 \cdot \text{h}^{-1}$  to  $1.5 \text{ m}^3 \cdot \text{h}^{-1}$ , the cooling capacity just decreased by 7%. These strong variations in the water flow would always introduce instabilities in the operation of the system.

## Conclusions

A single-effect ammonia/lithium nitrate absorption chiller was experimentally characterised at part-load. The chiller used brazed plate heat exchangers in all its thermal components, including the absorber and the generator. With a simple ON-OFF control the cooling capacity reacted fast in the same way as a conventional vapour compression machine did.

The part-load cycling degradation curve of the thermal coefficient of performance was quite similar to the part-load curves published in the open literature for ammonia/water absorption chillers.

The part-load curve of the electrical coefficient of performance was obtained by adjusting the experimental data to the curve shape proposed in the standards using the least square method. The degradation coefficient was 0.7985, which matched the value obtained by dividing the remaining electrical consumption generated during the OFF half cycles by the total energy consumption.

The ammonia/lithium nitrate absorption chiller was built using brazed plate heat exchangers and was agile with short transient response times, which were similar to those of vapour compression machines.

Finally, the experimental results published in this paper show that at part-load operation mode it is much more convenient to use an ON-OFF control to achieve a higher electrical coefficient of performance than to modify the hot water temperature.

### **Acknowledgements**

This work was co funded by the *Agencia de Innovación y Desarrollo de Andalucía*, ref: IDEA-351036, and the *Corporación Tecnológica de Andalucía*, ref: CTA-11/426 as part of the CONFISOL Project.

**References**

- [1] Albers J., Kuhn A., Petersen S., Ziegler F. Control of absorption chillers by insight: the characteristic equation. Proc. of 17<sup>th</sup> Int. Conf. on Process Engineering and Plant Design, Krakow Poland, 2008.
- [2] Anderson C. M. Control systems. United States Patent US3250084 A, Carrier Corp. 1966.
- [3] Bourouis M., Coronas A., Vallès M., Zamora M. Air/water or water/water absorption water cooler using ammonia and lithium nitrate, OEPM Madrid P200930758. 29/09/2009, PCT/ES2010/070608, 2009.
- [4] Chow T.T., Zhang G.Q., Lin Z., Song C. L. Global optimization of absorption chiller system by genetic algorithm and neural network. Energy and Buildings, 2002, 34,103-109
- [5] Clauß V., Kühn A., Ziegler F. A new control strategy for solar driven absorption chillers. 2nd International Conference Solar Air Conditioning Tarragona, Spain (2007)
- [6] Didion D., Radermacher R. Part-Load performance characteristics of residential absorption chillers and heat pumps. International Journal of Refrigeration, 1984, 7, 393-398
- [7] Henderson H., Yuang Y.J., Parker D. Residential equipment part load curves for use in DOE-2. Assistant Secretary for Energy Efficiency and Renewable Energy, Office of Building Technology, State and Community Programs, Office of Building Systems of the U.S. Department of Energy under Contract No. DE-AC03-76SF00098, 1999.

- [8] Jenkins N. Absorption chiller control logic. Patent WO2004063646 A1, Carrier Corporation 2003
- [9] Koeppel E.A., Mitchell J.W., Klein S.A., Flake, B.A. Optimal supervisory control of an absorption chiller system. HVAC and Research, 1995, 1, 325-342
- [10] Kühn A., Corrales Ciganda J.L., Ziegler F. Comparison of control strategies of solar absorption chillers. 1st International Conference on Heating, Cooling and Buildings, EUROSUN 2008, Lisbon, Portugal, 2008
- [11] Labus J., Korolija I., Marjonovic-Halburg L., Zhang Y., Coronas A. ANN application to modelling and control of small absorption chillers. First Building and Optimization Conference, Loughborough, UK, 245-252, 2012.
- [12] Lazzarin R.M. Steady and transient behaviour of LiBr absorption chillers of low capacity. International Journal of Refrigeration, 1980, 3, 213-218
- [13] Lazzarin R.M. Solar cooling plants: How to arrange solar collectors, absorption chillers and the load. International Journal of Low Carbon Technologies, 2007a, 2, 376-390.
- [14] Lazzarin R.M. Solar cooling plants: Some characteristic system arrangements. International Journal of Low Carbon Technologies, 2007b, 2, 391-404
- [15] Mann L.J., Stewart D.O. Refrigerating apparatus. United States Patent US3099139 A, General Motors Corp., 1963
- [16] Ogawa A., Hitomi K., Maekawa M., Yoshii K., Arima H. and Enomoto, E. Control system for absorption refrigerator. United States Patent 5,138,846. Sanyo Electric Co., Ltd. (Osaka, JP), 1992

- [17] Park C.W., Jeong J.H., Kang Y.T. Energy consumption characteristics of an absorption chiller during the partial load operation. *International Journal of Refrigeration*, 2004, 27, 948–954
- [18] Pérez de Viñaspre M., Bourouis M., Coronas A., García A., Soto V., Pinazo J.M. Monitoring and analysis of an absorption air-conditioning system. *Energy and Buildings*, 2004, 36, 933-943
- [19] Rotartica. Rotartica Solar 045, Installation and Maintenance Manual, Rotartica, S.A, 2007
- [20] Chilli. Chilli PSC12 12kW absorption chiller, Operating instructions/Installation manual, SolarNext AG, Nordstrase 10, 83253 Rimsting,DE, 2008
- [21] Storckenmaier F., Harm M., Schweigler C., Ziegler F., Albers J., Kohlenbach P., Sengewald T. 2003. Small capacity water/LiBr absorption chiller for solar cooling and waste heat driven cooling. *International Congress of Refrigeration*, Washington, D.C, USA, 2003
- [22] Sun D.W. Comparison of the performances of  $\text{NH}_3\text{-H}_2\text{O}$ ,  $\text{NH}_3\text{-LiNO}_3$ , and  $\text{NH}_3\text{-NaSCN}$  absorption refrigeration systems. *Energy Conversion Management*, 1998, 39, 357-358
- [23] Yazaki. YAZAKI 10, 20 and 30 RT S-series water fired single-effect absorption chiller /chiller-heater, Yazaki Energy Systems, Inc., 701 E. Plano Parkway, Suite 305, Plano, TX 75073-6700, 2009
- [24] Yeung M.R., Yuen P.K., Dunn A., Cornish L.S. Performance of a solar powered air conditioning system in Hong Kong. *Solar Energy*, 1992, 48, 309-319

- [25] Zacarias A., Venegas M., Ventas R., Leucona A. Experimental assessment of ammonia adiabatic absorption into ammonia-lithium nitrate solution using a flat fan nozzle. *Applied Thermal Engineering*, 2011, 31, 3569-3579
- [26] Zamora M., Bourouis M., Coronas A., Vallès M. Pre-industrial development and experimental characterization of a new air-cooled and water-cooled ammonia/lithium nitrate absorption chillers. *International Journal of Refrigeration*, 2014, 45, 189-197.
- [27] Zamora M. Industrial optimization and control strategy of an air-cooled ammonia / lithium nitrate absorption chiller (in Spanish), PhD University Rovira i Virgili, 2012.

Table 1 - Part load test matrix

	PLR (%)	$T_{AC1}$ (°C) <sup>a</sup>	$\Delta T_C$ (°C) <sup>b</sup>	$T_{E2}$ (°C)	$T_{G1}$ (°C) <sup>c</sup>
A	100	35	$\Delta T_{CN}$	15.5	90
B	75	35	$\Delta T_{CN} \cdot 0.75$	15.5	90
C	50	35	$\Delta T_{CN} \cdot 0.50$	15.5	90
D	25	35	$\Delta T_{CN} \cdot 0.25$	15.5	90

$$^a \dot{V}_{AC} = 6 \text{ m}^3 \cdot \text{h}^{-1}$$

$$^b \dot{V}_E = 2 \text{ m}^3 \cdot \text{h}^{-1}$$

$$^c \dot{V}_G = 3 \text{ m}^3 \cdot \text{h}^{-1}$$

Table 2 - Circulation pump power consumption

Pumping power (prEN 14511-3:2011)					
	$\dot{V}$ (m <sup>3</sup> ·h <sup>-1</sup> )	$\Delta P_w$ (bar)	$P_{w_{hyd}}$ (W) <sup>*</sup>	$\eta$	$P_{w_{pump}}$ (W)
Evaporator water circuit	2	0.231	12.83	0.16	79 <sup>**</sup>
Generator water circuit	3	0.3	25	0.2	125
Cooling water circuit	6	0.3	50.0	0.25	200

<sup>\*</sup> Hydraulic power of the circulation water pump due to pressure drop in a heat exchanger

<sup>\*\*</sup> This value must be subtracted from the cooling capacity value

Table 3 - Testing results at full capacity (PLR of 100%)

Test at full capacity		
$T_{G1} = 90 \text{ }^\circ\text{C}$ ; $T_{AC1} = 35 \text{ }^\circ\text{C}$		
$\dot{V}_E = 2 \text{ m}^3 \cdot \text{h}^{-1}$ ; $\dot{V}_G = 3 \text{ m}^3 \cdot \text{h}^{-1}$ ; $\dot{V}_{AC} = 6 \text{ m}^3 \cdot \text{h}^{-1}$		
	$T_{E2} = 15.5 \text{ }^\circ\text{C}$	$T_{E2} = 8.5 \text{ }^\circ\text{C}$
$\Delta T_E = T_{E1} - T_{E2} \text{ (}^\circ\text{C)}$	4.3	3.2
Cooling capacity (kW)	10.1	7.5
Generation power (kW)	16.6	13.4
Chiller power consumption (kW)	0.38	0.38
$\text{COP}_{\text{ther}} \text{ (-)}$	0.61	0.56
$\text{COP}_{\text{elec}} \text{ (-)}$	26.58	19.74
Chilled water pump consumption (prEN 14511-3:2011) (kW)	0.079	0.079
Generation water pump consumption (prEN 14511-3:2011) (kW)	0.125	0.125
Cooling water pump consumption (prEN 14511-3:2011) (kW)	0.200	0.200
Cooling capacity (prEN 14511-3:2011) (kW)	9.9	7.4
Total power consumption (prEN 14511-3:2011) (kW)	0.784	0.784
$\text{COP}_{\text{ther}} \text{ (prEN 14511-3:2011) (-)}$	0.60	0.55
$\text{COP}_{\text{elec}} \text{ (prEN 14511-3:2011) (-)}$	12.63	9.44

Table 4 - Testing results at part loads of 25%, 50% and 75% and chilled water temperature of 15.5 °C.

$T_{E2} = 15.5\text{ °C}$ ; $T_{G1} = 90\text{ °C}$ ; $T_{AC1} = 35\text{ °C}$			
$\dot{V}_E = 2\text{ m}^3\cdot\text{h}^{-1}$ ; $\dot{V}_G = 3\text{ m}^3\cdot\text{h}^{-1}$ ; $\dot{V}_{AC} = 6\text{ m}^3\cdot\text{h}^{-1}$			
Part load (%)	75	50	25
Load (kW)	7.5	5.0	3.1
$T_{E2}$ (°C)	15.3	16.0	16.3
Number of steady state periods considered (n)	1	3	2
Cooling energy (kWh)	6.39	9.87	3.85
Generation energy (kWh)	10.94	17.61	7.04
Electric energy consumed by the chiller (kWh)	0.25	0.44	0.18
Cooling energy (prEN 14511-3:2011) (kWh)	6.33	9.73	3.75
Electric energy (prEN 14511-3:2011) (kWh)	0.53	0.95	0.43
Actual PLR (%)	80	55	30
$COP_{ther}$ (-)	0.58	0.56	0.55
$COP_{elec}$ (-)	25.56	22.43	21.39
$COP_{ther}$ (prEN 14511-3:2011) (-)	0.58	0.55	0.53
$COP_{elec}$ (prEN 14511-3:2011) (-)	11.94	10.24	8.72

Table 5- Test results at part load of 50% and chilled water temperature of 8.5 °C.

$T_{E2} = 8.5 \text{ °C} ; T_{G1} = 90 \text{ °C} ; T_{AC1} = 35 \text{ °C}$ $\dot{V}_E = 2 \text{ m}^3 \cdot \text{h}^{-1} ; \dot{V}_G = 3 \text{ m}^3 \cdot \text{h}^{-1} ; \dot{V}_{AC} = 6 \text{ m}^3 \cdot \text{h}^{-1}$	
Part load (%)	50
Load (kW)	3.5
$T_{E2}$ (°C)	8.5
Number of steady state periods considered (n)	3
Cooling energy supplied by the chiller (kWh)	10.16
Generation energy consumed by the chiller (kWh)	19.29
Electric energy consumed by the chiller (kWh)	0.55
Cooling energy (prEN 14511-3:2011) (kWh)	9.97
Electric energy (prEN 14511-3:2011) (kWh)	1.18
Actual PLR (%)	57
$\text{COP}_{\text{ther}}$ (-)	0.53
$\text{COP}_{\text{elec}}$ (-)	18.47
$\text{COP}_{\text{ther}}$ (prEN 14511-3:2011) (-)	0.52
$\text{COP}_{\text{elec}}$ (prEN 14511-3:2011) (-)	8.45

Table 6 - Thermal and electrical coefficients of performance referred to full capacity values

$T_{E2} = 15.5 \text{ }^\circ\text{C}$ ; $T_{G1} = 90 \text{ }^\circ\text{C}$ ; $T_{AC1} = 35 \text{ }^\circ\text{C}$ $\dot{V}_E = 2 \text{ m}^3 \cdot \text{h}^{-1}$ ; $\dot{V}_G = 3 \text{ m}^3 \cdot \text{h}^{-1}$ ; $\dot{V}_{AC} = 6 \text{ m}^3 \cdot \text{h}^{-1}$				
PLR (%)	$\text{COP}_{\text{ther}} (-)$	$\text{COP}_{\text{ther}} / \text{COP}_{\text{therN}}$	$\text{COP}_{\text{elec}} (-)$	$\text{COP}_{\text{elec}} / \text{COP}_{\text{elecN}}$
100	0.60	1	12.63	1
80	0.58	0.97	11.94	0.95
55	0.55	0.92	10.24	0.81
30	0.53	0.88	8.72	0.69
$T_{E2} = 8.5 \text{ }^\circ\text{C}$ ; $T_{G1} = 90 \text{ }^\circ\text{C}$ ; $T_{AC1} = 35 \text{ }^\circ\text{C}$ $\dot{V}_E = 2 \text{ m}^3/\text{h}$ ; $\dot{V}_G = 3 \text{ m}^3/\text{h}$ ; $\dot{V}_{AC} = 6 \text{ m}^3/\text{h}$				
PLR (%)	$\text{COP}_{\text{ther}} (-)$	$\text{COP}_{\text{ther}} / \text{COP}_{\text{therN}}$	$\text{COP}_{\text{elec}} (-)$	$\text{COP}_{\text{elec}} / \text{COP}_{\text{elecN}}$
100	0.55	1	9.44	1
57	0.52	0.95	8.45	0.90

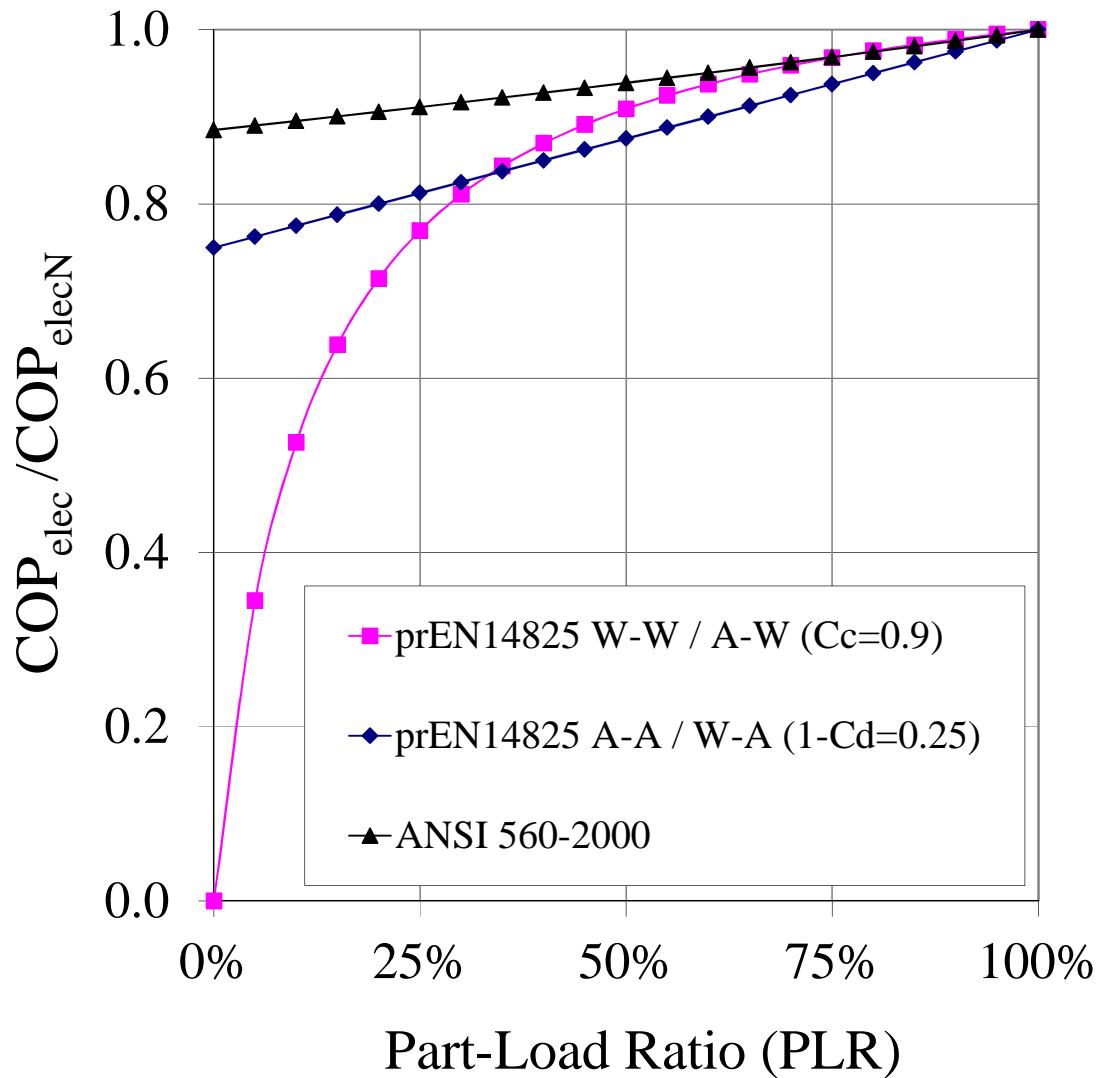


Fig. 1 - Part-load COP cycling degradation curve for the vapour compression equipment (prEN-14825:2011) and for the water/lithium bromide absorption chillers (ANSI/ARI 560:2000)

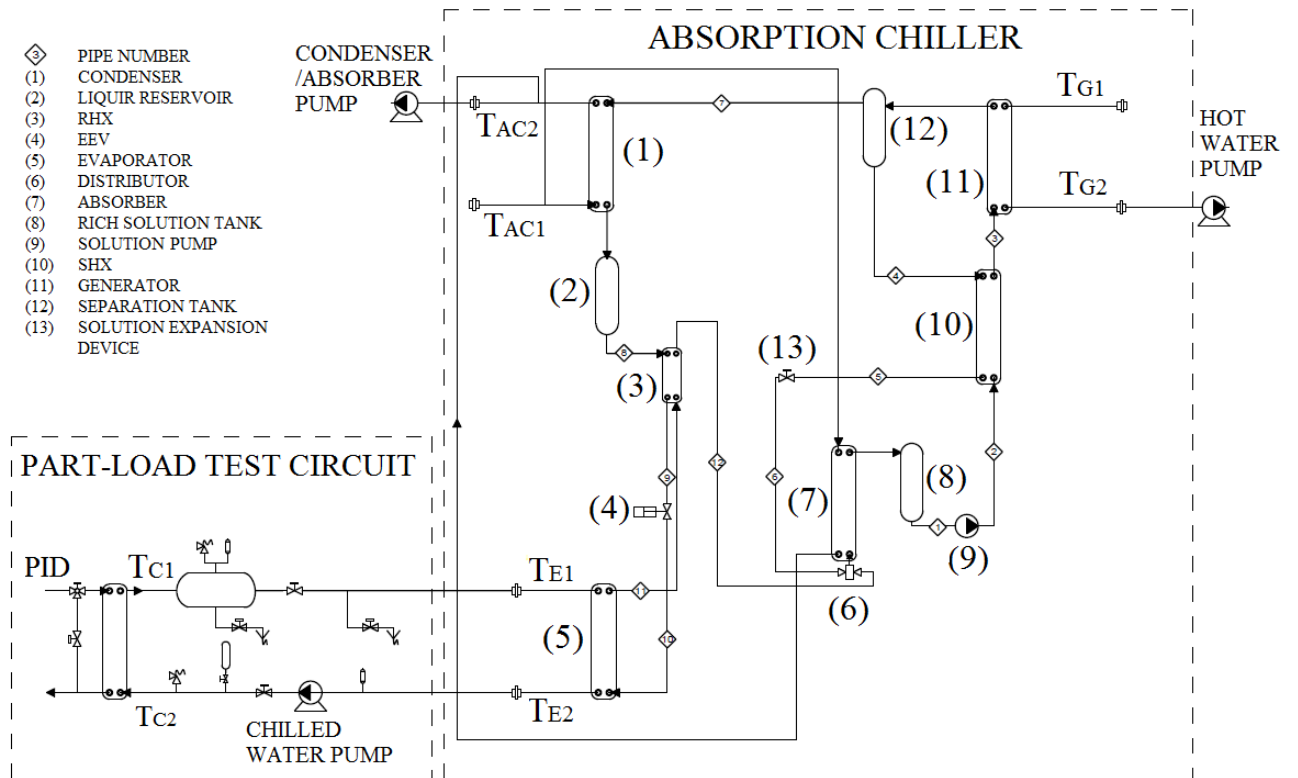


Fig. 2 - Test bench for part-load measurements implemented in the CREVER laboratory

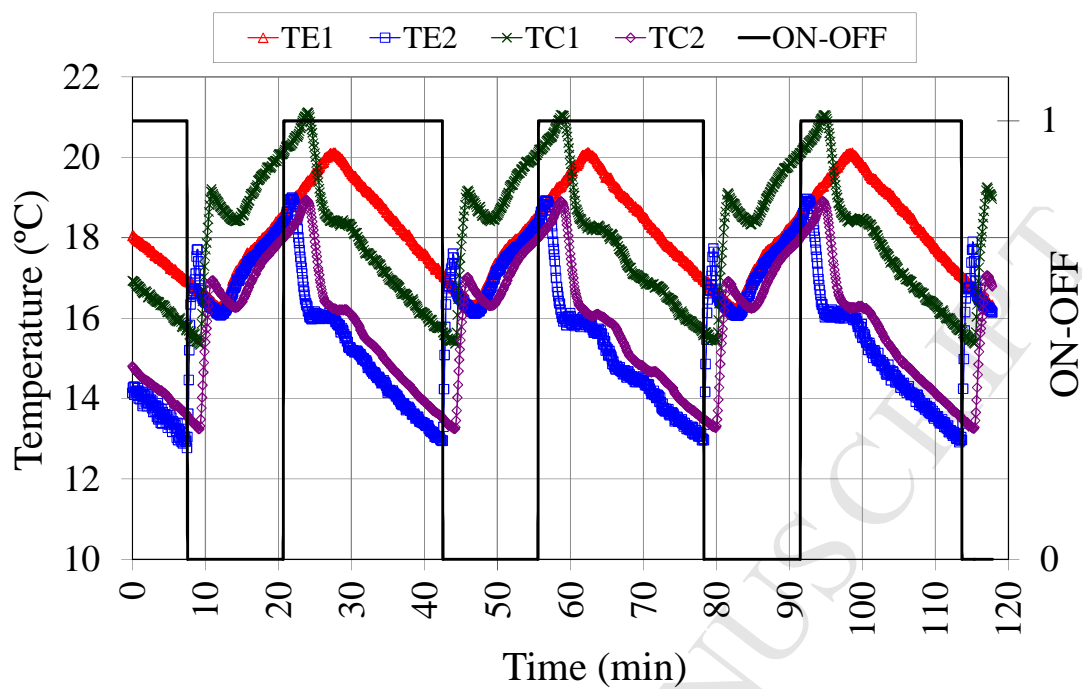


Fig. 3 - Temperature profiles at PLR of 50% and chilled water temperature of 15.5 °C

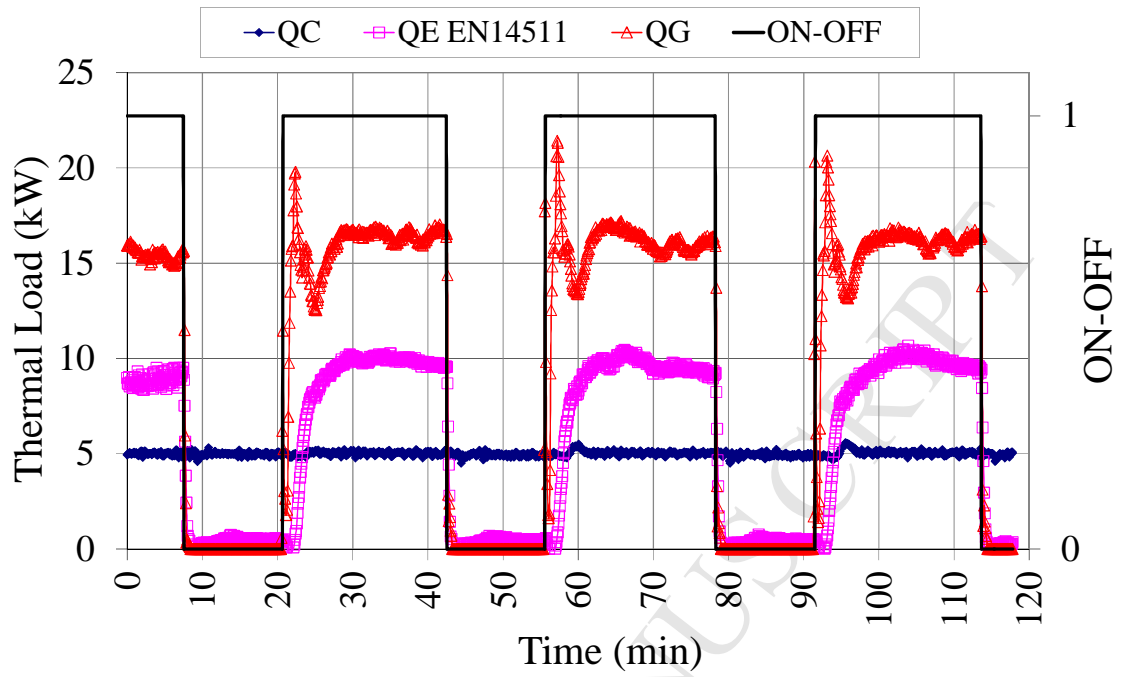


Fig. 4 - Thermal loads at PLR of 50%: Cooling load ( $\dot{Q}_C$ ), cooling capacity ( $\dot{Q}_E$ ) and generation power ( $\dot{Q}_G$ ), at chilled water temperature of 15.5 °C

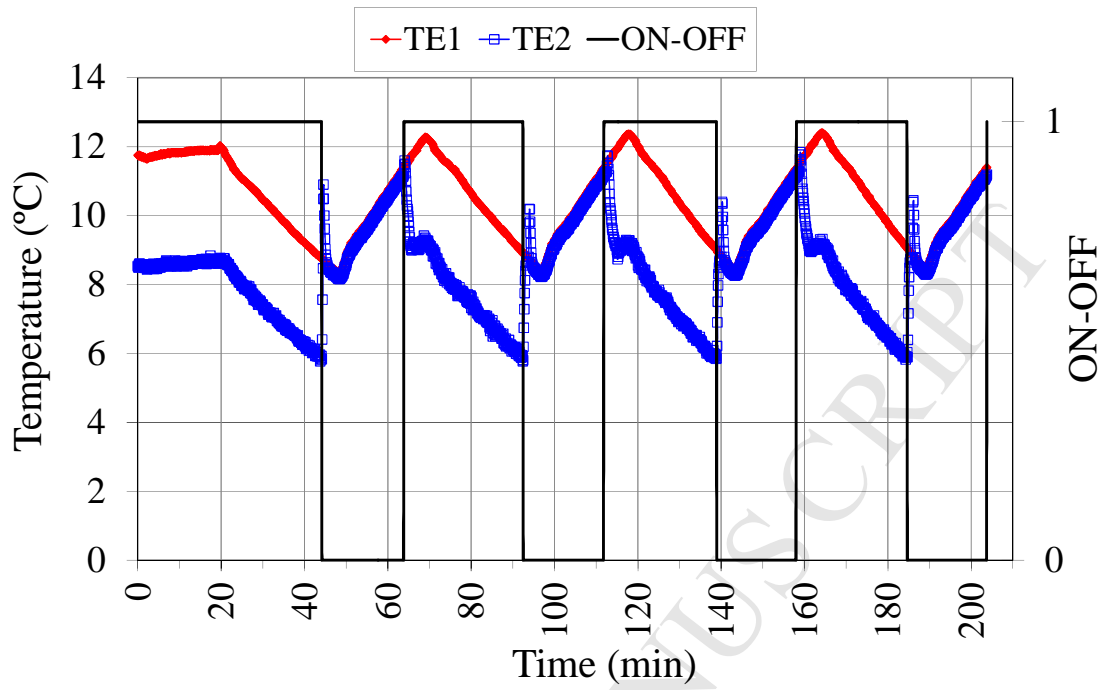


Fig. 5 - Temperature profiles at PLR of 50% and chilled water temperature of 8.5 °C

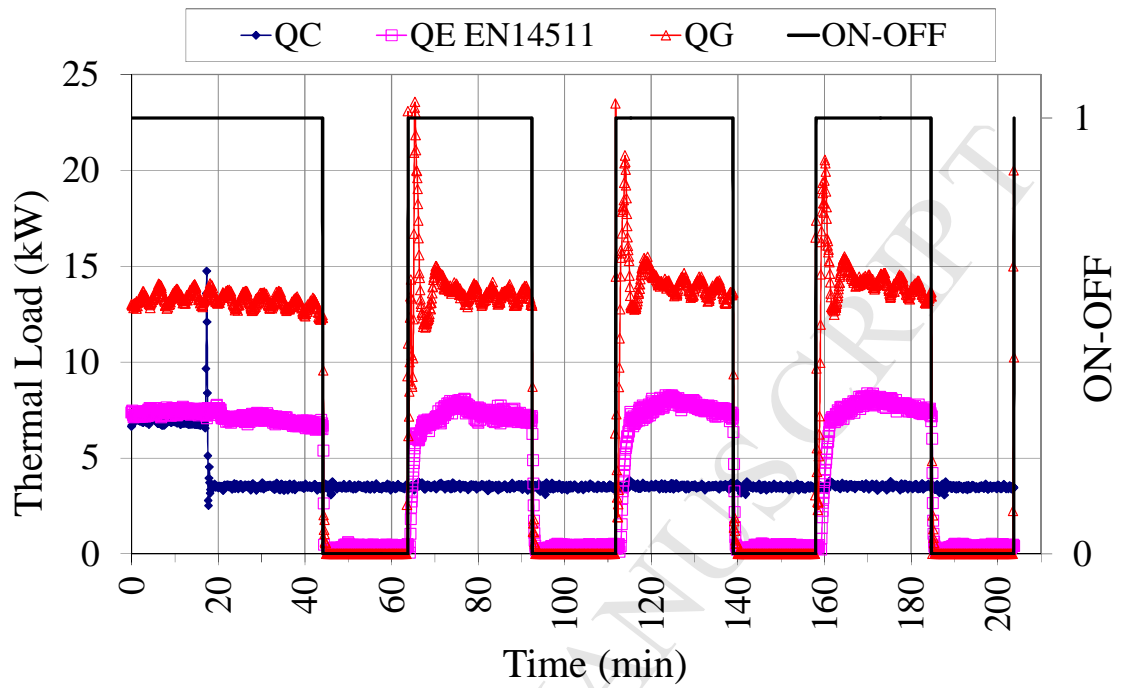


Fig. 6 - Thermal loads at PLR of 50%: cooling load ( $\dot{Q}_C$ ), cooling capacity ( $\dot{Q}_E$ ) and generation power ( $\dot{Q}_G$ ) at chilled water temperature of 8.5 °C

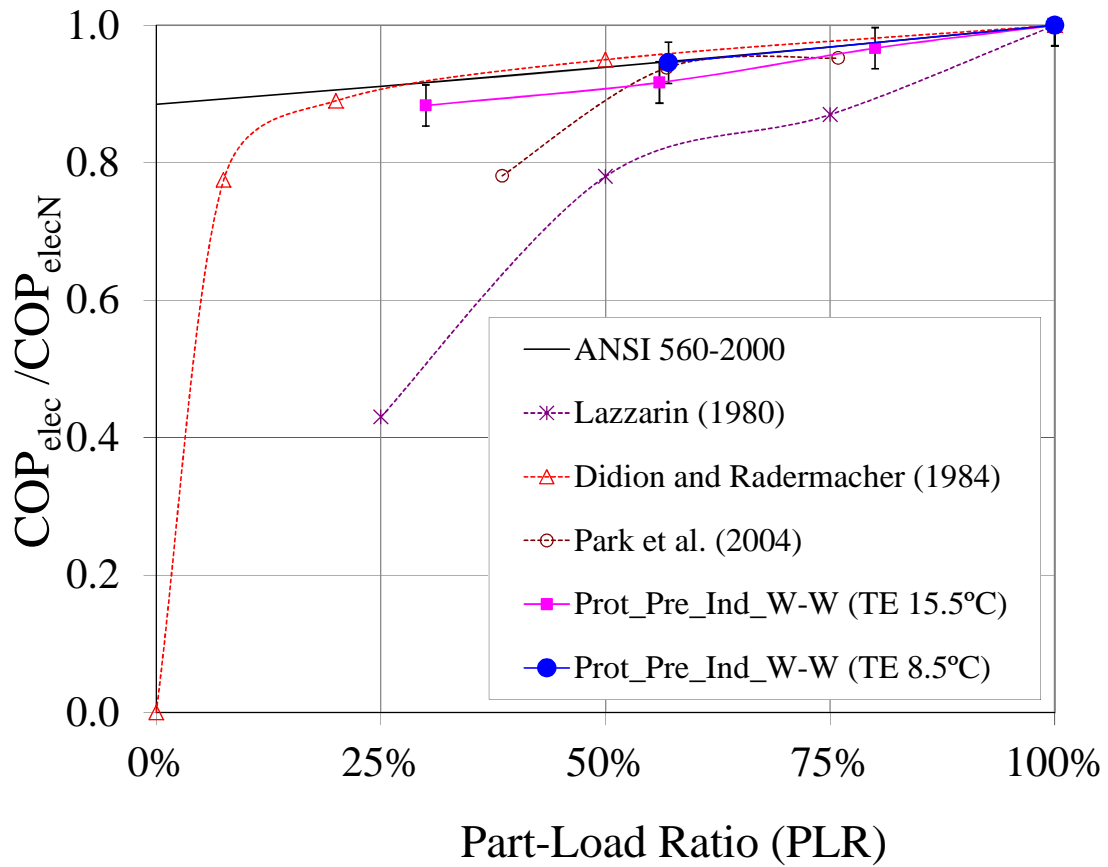


Fig. 7 - Thermal COP part-load cycling degradation curve

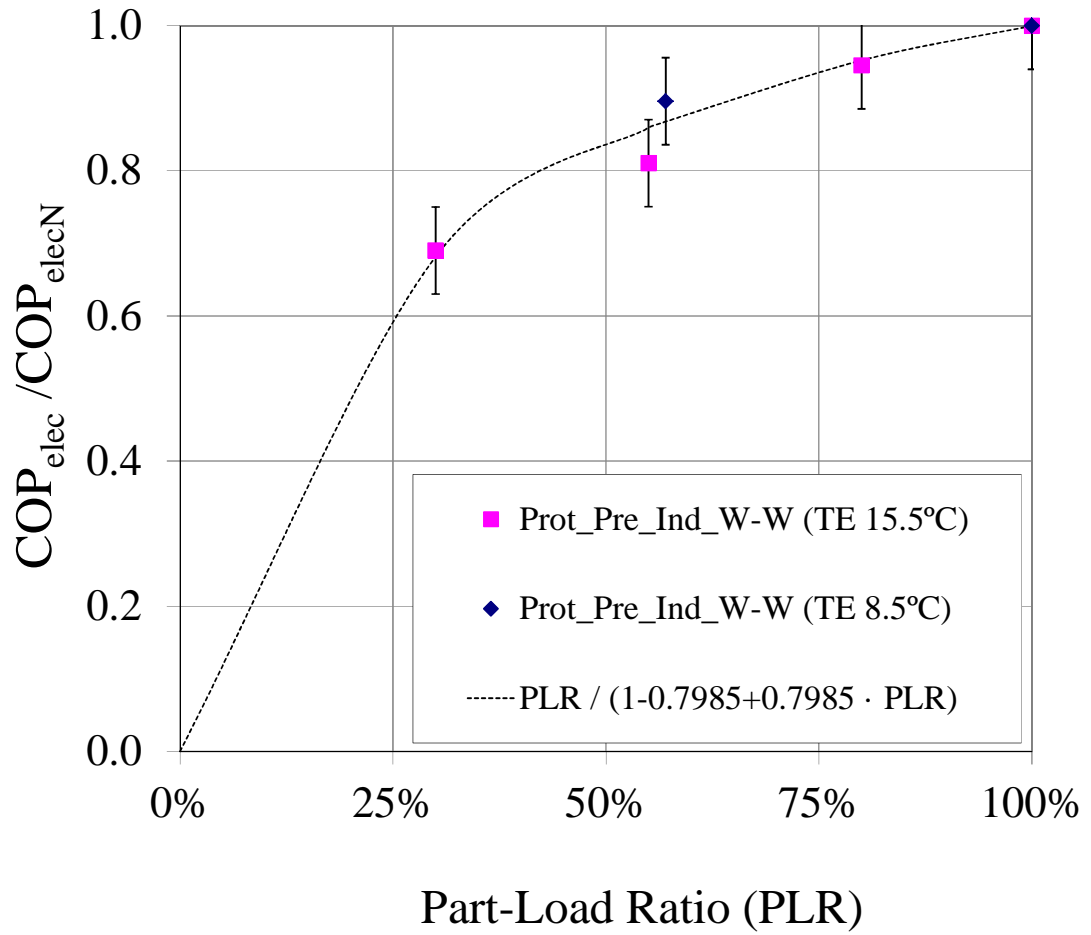


Fig. 8 - Electrical COP part-load cycling degradation curve

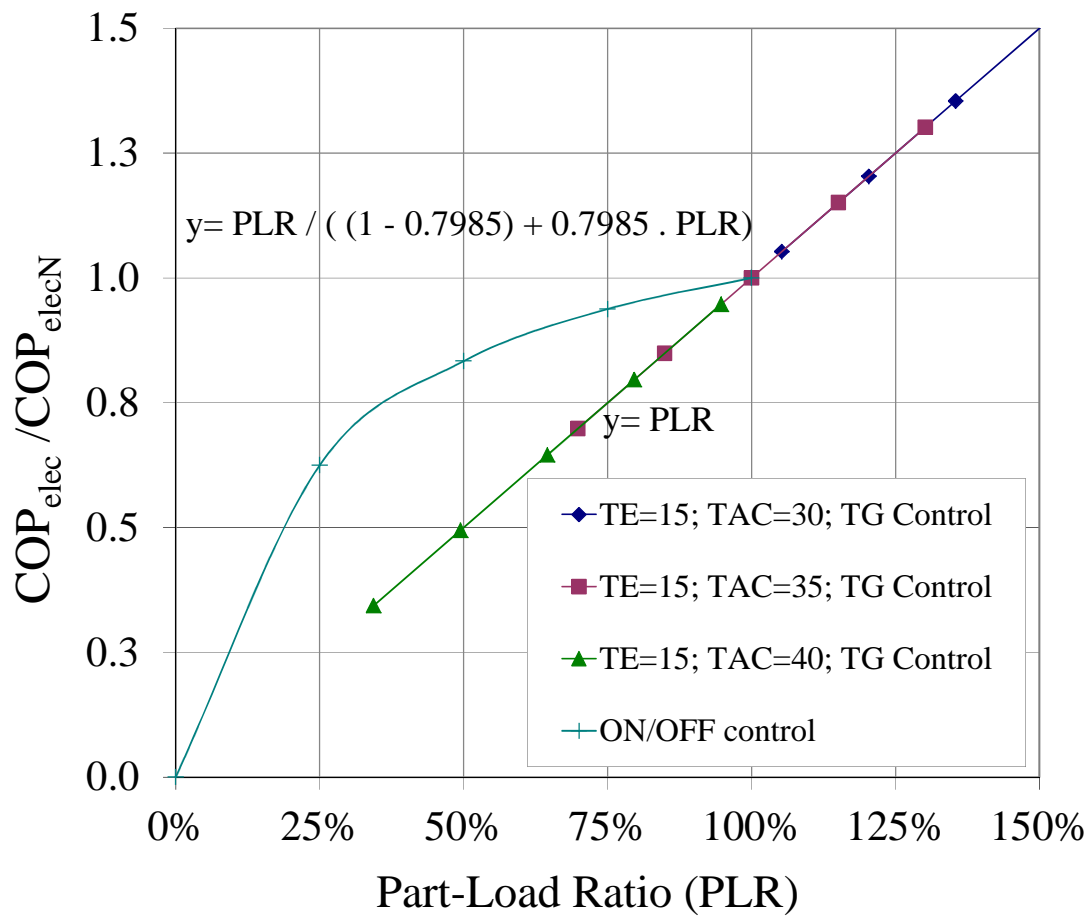


Fig. 9 - Electrical COP part-load degradation curve for ON-OFF control and hot water control

**Figures caption**

Fig. 1 - Part-load COP cycling degradation curve for the vapour compression equipment (prEN-14825:2011) and for the water/lithium bromide absorption chillers (ANSI/ARI 560:2000)

Fig. 2 - Test bench for part-load measurements implemented in the CREVER laboratory

Fig. 3 - Temperature profiles at PLR of 50% and chilled water temperature of 15.5 °C

Fig. 4 - Thermal loads at PLR of 50%: Cooling load ( $\dot{Q}_C$ ), cooling capacity ( $\dot{Q}_E$ ) and generation power ( $\dot{Q}_G$ ) at chilled water temperature of 15.5 °C

Fig. 5 - Temperature profiles at PLR of 50% and chilled water temperature of 8.5 °C

Fig. 6 - Thermal loads at PLR of 50%: cooling load ( $\dot{Q}_C$ ), cooling capacity ( $\dot{Q}_E$ ) and generation power ( $\dot{Q}_G$ ) at chilled water temperature of 8.5 °C

Fig. 7 - Thermal COP part-load cycling degradation curve

Fig. 8 - Electrical COP part-load cycling degradation curve

Fig. 9 - Electrical COP part-load degradation curve for ON-OFF control and hot water control

**Highlights**

- A new  $\text{NH}_3/\text{LiNO}_3$  absorption chiller was experimentally characterized at part-load
- Thermal and electrical coefficients of performance at part-load were obtained
- Degradation of the electrical COP operating with an ON-OFF control was analyzed
- The chiller presented a fast response due to the use of plate heat exchangers